2021 60th IEEE Conference on Decision and Control (CDC)
December 13-15, 2021. Austin, Texas

The Free Response of an Identified Model of a Linear System with a Completely Unknown Harmonic Disturbance Exactly Forcasts the Free-Plus-Forced Response of the True System Thereby Enabling Adaptive MPC for Harmonic Disturbance Rejection

Syed Aseem Ul Islam, Khaled Aljanaideh, Tam W. Nguyen,
Ilya V. Kolmanovsky, and Dennis S. Bernstein

***Abstract*— This paper considers system identification in the presence of an unmeasured, unknown, and unmatched multi-tone harmonic disturbance with completely unknown spectrum. It is shown that the identified model possesses spurious poles at the disturbance frequencies that are cancelled by coincident, spurious zeros. Although the presence of the spurious poles is expected, this paper shows that the free response of the identified model is identical—*in frequencies, amplitudes, and phases*—to the free-plus-forced response of the true system. Consequently, by retaining—rather than cancelling—the coincident, spurious poles and zeros, the identified model has the ability to forecast the future response to an unknown harmonic input over a prediction horizon during which the harmonic disturbance persists. A numerical example illustrates the usefulness of this property to model predictive control with concurrent system identification for rejecting unmeasured, unknown, and unmatched harmonic disturbances with completely unknown spectrum.**

I. Introduction

One of the main challenges to system identification is unmeasured and unknown disturbances with unknown spectrum, which degrades the accuracy of the identified model. One of the goals of research in system identification is thus to mitigate the impact of these signals on the achievable model accuracy. The present paper investigates a surprising phenomenon that not only contradicts this belief, but clearly shows that the "corruption" of the identified model by the unmodeled disturbance actually enhances the predictive ability of the identified model with substantial benefits for model predictive control.

For system identification in the presence of an unknown sinusoidal disturbance, this paper shows that the identified model possesses spurious poles at the disturbance frequency that are cancelled by coincident, spurious zeros. Although the presence of these spurious poles is expected, the main result of this paper shows that the free response of the identified model is identical—*in frequencies, amplitudes, and phases*—to the free-plus-forced response of the true system. Consequently, by retaining—rather than cancelling—the coincident, spurious poles and zeros, the identified model has the ability to forecast the future response to an unknown harmonic input with completely unknown spectrum.

Syed Aseem Ul Islam, Tam W. Nguyen, Ilya V. Kolmanovsky, and Dennis S. Bernstein are with the Department of Aerospace Engineering, University of Michigan, Ann Arbor, MI, USA. aseemisl@umich.edu, tamwilly.nguyen@gmail.com, dsbaero@umich.edu, and Khaled Aljanaideh is at Jordan University of Science and Technology, Irbid, Jordan kfaljanaideh@just.edu.jo.

The ability of the identified model to correctly forecast the future free-plus-forced response of the true system has fundamental implications for harmonic disturbance rejection when the disturbance spectrum is unknown but is stationary or slowly changing. This problem has been widely studied using a wide variety of methods, for example, [1], [2]. In contrast, classical internal model control requires prior knowledge of the frequency content of the harmonic disturbance [3].

The present paper is motivated by predictive cost adaptive control (PCAC) [4]–[6] for unmeasured, unknown, and unmatched harmonic disturbances with unknown spectrum. This approach employs online linear system identification using recursive least squares. The linear system is assumed to be disturbed by an unmeasured harmonic signal with unknown frequencies, amplitudes, and phases. Since the plant input consists of the known control input and the unmodeled harmonic disturbance, it follows that the output is corrupted by the response to the harmonic disturbance. Consequently, the regression is based on an erroneous input signal as well as a corrupted output signal.

Because of the unmodeled harmonic disturbance, the identified model includes pairs of complex conjugate poles at the disturbance frequencies that are canceled by pairs of coincident complex conjugate zeros. Normally, coincident, spurious poles and zeros would be removed from the identified model. What is surprising, however, is the fact that, with initial conditions provided by prior inputs and outputs, the free response of the identified model exactly forecasts the free-plus-forced response of the true system with the harmonic disturbance. The present paper proves this fact for first- and second-order systems with a single-tone harmonic disturbance and demonstrates that the ability to forecast the free-plus-forced response of the true system with the harmonic disturbance enables MPC to reject the harmonic disturbance despite the fact that it is unmeasured, unmatched, and unknown with completely unknown spectrum.

II. A Surprising Feature of the Identified Model

In this section, we illustrate the phenomenon described in the previous section. As an illustrative example, consider the

978-1-6654-3658-8/21/$31.00 ©2021 IEEE

SISO system

$$y_k = G(\mathbf{q})(u_k + w_k), \tag{1}$$

where G is given by

$$G(\mathbf{q}) = \frac{\mathbf{q} - 0.3}{\mathbf{q}^2 - 1.4\mathbf{q} + 0.58}. \tag{2}$$

Note that, unlike the Z-transform variable, the time-domain, forward-shift operator $\mathbf{q}$ captures the effect of nonzero initial conditions without an additional term that displays the initial condition. This distinction is discussed in [7].

The *true system* (1) is driven by the sum of a Gaussian white-noise signal $u_k \sim \mathcal{N}(0, 10)$ and an unmodeled sinusoid $w_k = \sin 0.5k$. The system (1) is simulated for $k \in [0, 1000]$, and samples of y_k and u_k are used to fit the coefficients of G. Note that, since w_k is unmodeled, the input data u_k used for regression are erroneous, and the output data y_k are corrupted by w_k.

Although the model order is 2, we choose a 4th-order model structure; using recursive least squares [8], the poles and zeros of the identified model are shown in Figure 1. As can be seen, the identified model correctly estimates the poles and zeros of the true system. However, a pair of complex conjugate poles on the unit circle are also evident; these poles, which are accommodated by the model-order overparameterization, are not present in the true system and thus are spurious. In addition, the pair of complex conjugate poles are coincident with the spurious zeros. Close examination reveals that the frequency of the spurious pole/zero pairs is precisely the frequency of the unmodeled disturbance.

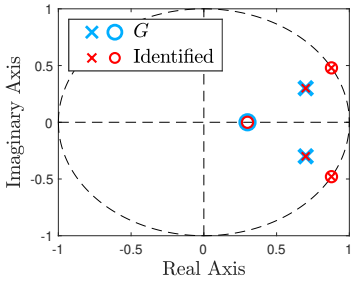

Fig. 1. Poles and zeros of the true system G and the identified model.

Clearly, the spurious pole/zero pairs are an artifact of the unmodeled disturbance. Since the poles and zero of the true system are correctly identified, it appears that, upon cancellation of the spurious pole/zero pairs, an acceptable model is obtained. In fact, as shown below, a better strategy from the point of view of prediction is to retain the spurious pole/zero pairs.

Next, we simulate the identified model and compare its response to the response of the true system. The identified model and the true system are initialized with y_k, u_k data obtained from a window of length 4 steps prior the end of the previous simulation. In particular, without cancelling the spurious poles and zeros, the identified model is simulated with zero input, yielding the free response for the given initial data Alternatively, the true system is simulated with input consisting only of w_k and with u_k set to zero. The resulting response y_k of the true system is thus given by the sum of its free response and forced response with initial $y_k, u_k + w_k$ data obtained from a window of length 2 steps prior the end of the previous simulation and with w_k applied at all subsequent steps. Figure 2 shows that the response of the identified model and true system are identical. We examine this phenomenon in the next section.

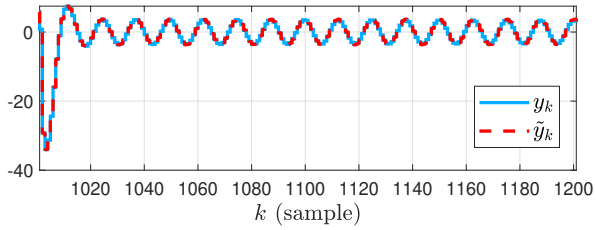

Fig. 2. This plot shows that the free response of identified model and the free-plus-forced response of the true system are identical. Note that, after the initial transients, which are identical, the steady-state harmonic responses are identical in frequency, amplitude, and phase.

III. Identified Models with Coincident Pole/Zero Pairs

Figures 1 and 2 suggest that the spurious poles and zeros that are present in the identified model and the initial condition determined by a prior window of data are somehow able to capture the forced response of the true system. To examine this phenomenon more closely, we refer to the spurious poles and zeros in the identified model as *coincident* poles and zeros in order to reflect the fact that they exactly cancel.

The following is the main result of this paper.

Proposition 1. Let G be a SISO transfer function of order n, and define $\tilde{G} \triangleq GG_{\mathrm{pz}}$, where G_{pz} is a transfer function of order $2n_\omega$ where

$$G_{\mathrm{pz}}(\mathbf{q}) \triangleq \prod_{i=1}^{n_\omega} \frac{\mathbf{q}^2 - 2\cos\omega_i \mathbf{q} + 1}{\mathbf{q}^2 - 2\cos\omega_i \mathbf{q} + 1}. \tag{3}$$

Furthermore, for all $k > k_b$, let y_k denote the response of G with initial condition determined by $y_{k_a}, \ldots, y_{k_b}$ and $u_{k_a} + w_{k_a}, \ldots, u_{k_b} + w_{k_b}$, and with input $u_{k_b+1} + w_{k_b+1}, \ldots, u_{k_0} + w_{k_0}$, where

$$w_k \triangleq \sum_{i=1}^{n_\omega} \gamma_i \sin\omega_i k, \tag{4}$$

$$k_a \triangleq k_0 - 2n - 2n_\omega + 1, \tag{5}$$

$$k_b \triangleq k_0 - n - 2n_\omega. \tag{6}$$

In addition, for all $k > k_0$ let $\tilde{y}_k$ denote free response of $\tilde{G}$ with initial condition determined by $y_{k_b+1}, \ldots, y_{k_0}$ and $u_{k_b+1}, \ldots, u_{k_0}$. Furthermore, for all $k > k_0$ let $u_k = 0$. Then, for all $k > k_0$, $\tilde{y}_k = y_k$.

IV. Proof of Proposition 1 for $n = 1$ and $n = 2$ with $n_\omega = 1$

In this section we prove Proposition 1 for first- and second-order transfer functions of the form

$$G_1(\mathbf{q}) = \frac{\beta_1}{\mathbf{q} + \alpha_1}, \tag{7}$$

$$G_2(\mathbf{q}) = \frac{\beta_1 \mathbf{q} + \beta_2}{\mathbf{q}^2 + \alpha_1 \mathbf{q} + \alpha_2}, \tag{8}$$

with a single harmonic disturbance. The proof involves the calculation of the free response of a transfer function G cascaded with coincident poles and zeros on the unit circle as well as the calculation of the free-plus-forced response of G, where the forcing is a harmonic signal whose frequency is the same as the frequency of the coincident poles and zeros. This calculation involves a sequence of initial steps leading to a recursion that is valid for all subsequent time steps. The proof thus entails showing that these sequences are identical.

We show the details for $n = 2$. The details in the case $n = 1$ are similar and simpler, and are thus omitted.

The proof of Proposition 1 uses the following identity.

Fact:

$$\sin(\alpha + 2)\omega \equiv 2\sin(\alpha + 1)\omega \cos\omega - \sin(\alpha)\omega. \tag{9}$$

Proof. Using $(\sin x)\cos y \equiv \frac{1}{2}[\sin(x - y) + \sin(x + y)]$ [9, p. 236]

$$\sin(\alpha + 1)\omega \cos\omega = \frac{1}{2}[\sin(\alpha + 1 + 1)\omega + \sin(\alpha + 1 - 1)\omega],$$

$$2\sin(\alpha + 1)\omega \cos\omega = \sin(\alpha + 2)\omega + \sin\alpha\omega,$$

$$\sin(\alpha + 2)\omega = 2\sin(\alpha + 1)\omega \cos\omega - \sin\alpha\omega. \square$$

A. Proof of Proposition 1 for $n = 2$

Consider the system

$$G(\mathbf{q}) = \frac{b_1 \mathbf{q} + b_2}{\mathbf{q}^2 + a_1 \mathbf{q} + a_2}. \tag{10}$$

The output y_k of (10) can be written as

$$y_{k+1} = \sum_{i=0}^{1} (b_{i+1} u_{k-i} + b_{i+1} w_{k-i} - a_{i+1} y_{k-i}). \tag{11}$$

The outputs y_{k_0-5}, y_{k_0-4} and inputs $u_{k_0-5}, \ldots, u_{k_0}$ are arbitrary, and

$$u_k = 0, \quad k > k_0. \tag{12}$$

The disturbance is $w_k = \gamma \sin\omega k$. Since γ can be absorbed into the b_i coefficients in (11), it follows that it suffices to use

$$w_k = \sin\omega k, \tag{13}$$

for the proof.

It follows from (11)–(13) that for $k_0 - 4 \le k < k_0$

$$y_{k+1} = \sum_{i=0}^{1} [b_{i+1} u_{k-i} + b_{i+1} \sin\omega(k - i) - a_{i+1} y_{k-i}], \tag{14}$$

for $k_0 \le k < k_0 + 2$

$$y_{k_0+1} = -a_1 y_{k_0} - a_2 y_{k_0-1} + b_1 u_{k_0} + b_1 \sin\omega(k_0) + b_2 u_{k_0-1} + b_2 \sin\omega(k_0 - 1), \tag{15}$$

$$y_{k_0+2} = -a_1 y_{k_0+1} - a_2 y_{k_0} + b_1 \sin\omega(k_0 + 1) + b_2 u_{k_0} + \sin b_2\omega(k_0), \tag{16}$$

and for $k \ge k_0 + 2$

$$y_{k+1} = \sum_{i=0}^{1} [b_{i+1} \sin\omega(k - i) - a_{i+1} y_{k-i}]. \tag{17}$$

Next, consider the cascaded system

$$\tilde{G}(\mathbf{q}) = G(\mathbf{q}) \frac{\mathbf{q}^2 - 2\cos\omega\mathbf{q} + 1}{\mathbf{q}^2 - 2\cos\omega\mathbf{q} + 1}, \tag{18}$$

whose output $\tilde{y}_k$ can be written as

$$(\mathbf{q}^2 - 2\cos\omega\mathbf{q} + 1)\tilde{y}_{k+1} = (\mathbf{q}^2 - 2\cos\omega\mathbf{q} + 1) \cdot (-a_1\tilde{y}_k - a_2\tilde{y}_{k-1} + b_1 u_k + b_2 u_{k-1})$$

$$\tilde{y}_{k+1} = 2\tilde{y}_k \cos\omega - \tilde{y}_{k-1} + \sum_{i=0}^{1} b_{i+1}(u_{k-i} - 2u_{k-1-i}\cos\omega + u_{k-2-i}) + \sum_{i=0}^{1} a_{i+1}(2\tilde{y}_{k-1-i}\cos\omega - \tilde{y}_{k-i} - \tilde{y}_{k-2-i}). \tag{19}$$

Setting $k = k_0$ in (19) yields

$$\begin{aligned}\tilde{y}_{k_0+1} = {} & -a_1 y_{k_0} - a_2 y_{k_0-1} + b_1 u_{k_0} + b_2 u_{k_0-1} \\ & + 2y_{k_0}\cos\omega - y_{k_0-1} + 2a_1 y_{k_0-1}\cos\omega \\ & + 2a_2 y_{k_0-2}\cos\omega - 2b_1 u_{k_0-1}\cos\omega \\ & - 2b_2 u_{k_0-2}\cos\omega - a_1 y_{k_0-2} - a_2 y_{k_0-3} \\ & + b_1 u_{k_0-2} + b_2 u_{k_0-3}.\end{aligned} \tag{20}$$

Substituting for y_{k_0-1} in the 6th term in (20) using (14) yields

$$\begin{aligned}\tilde{y}_{k_0+1} = {} & -a_1 y_{k_0} - a_2 y_{k_0-1} + b_1 u_{k_0} + b_2 u_{k_0-1} \\ & + 2y_{k_0}\cos\omega - b_1 \sin\omega(k_0 - 2) - b_2 \sin\omega(k_0 - 3) \\ & + 2a_1 y_{k_0-1}\cos\omega + 2a_2 y_{k_0-2}\cos\omega \\ & - 2b_1 u_{k_0-1}\cos\omega - 2b_2 u_{k_0-2}\cos\omega.\end{aligned} \tag{21}$$

Substituting for y_{k_0} in the 4th term in (21) using (14) yields

$$\begin{aligned}\tilde{y}_{k_0+1} = {} & -a_1 y_{k_0} - a_2 y_{k_0-1} + b_1 u_{k_0} + b_2 u_{k_0-1} \\ & + 2b_1 \sin\omega(k_0 - 1)\cos\omega - b_1 \sin\omega(k_0 - 2) \\ & + 2b_2 \sin\omega(k_0 - 2)\cos\omega - b_2 \sin\omega(k_0 - 3).\end{aligned} \tag{22}$$

Using (9) and (15) in (22) yields

$$\begin{aligned}\tilde{y}_{k_0+1} = {} & -a_1 y_{k_0} - a_2 y_{k_0-1} + b_1 u_{k_0} + b_2 u_{k_0-1} \\ & + b_1 \sin\omega(k_0) + b_2 \sin\omega(k_0 - 1) \\ = {} & y_{k_0+1}.\end{aligned} \tag{23}$$

Using (12), (23), and setting $k = k_0 + 1$ in (19) yields

$$\begin{aligned}\tilde{y}_{k_0+2} &= -a_1 y_{k_0+1} - a_2 y_{k_0} + b_2 u_{k_0} + 2y_{k_0+1}\cos\omega \\ &\quad - y_{k_0} + 2a_1 y_{k_0} + 2a_2 y_{k_0-1}\cos\omega - 2b_1 u_{k_0}\cos\omega \\ &\quad - 2b_2 u_{k_0-1}\cos\omega - a_1 y_{k_0-1} - a_2 y_{k_0-2} \\ &\quad + b_1 u_{k_0-1} + b_2 u_{k_0-2}. \end{aligned} \tag{24}$$

Substituting for y_{k_0} and y_{k_0+1} in the 5th and 4th terms in (24), using (14) and (15), respectively, yields

$$\begin{aligned}\tilde{y}_{k_0+2} &= -a_1 y_{k_0+1} - a_2 y_{k_0} + b_2 u_{k_0} + 2b_1 \sin\omega(k_0)\cos\omega \\ &\quad - b_1 \sin\omega(k_0-1) + 2b_2 \sin\omega(k_0-1)\cos\omega \\ &\quad - b_2 \sin\omega(k_0-2). \end{aligned} \tag{25}$$

Using (9) and (16) in (25) yields

$$\begin{aligned}\tilde{y}_{k_0+2} &= -a_1 y_{k_0+1} - a_2 y_{k_0} + b_2 u_{k_0} \\ &\quad + b_1 \sin\omega(k_0+1) + b_2 \sin\omega(k_0) \\ &= y_{k_0+2}. \end{aligned} \tag{26}$$

Using (12), (23), (26), and setting $k = k_0 + 2$ in (19) yields

$$\begin{aligned}\tilde{y}_{k_0+3} &= -a_1 y_{k_0+2} - a_2 y_{k_0+1} + 2y_{k_0+2}\cos\omega - y_{k_0+1} \\ &\quad + 2a_1 y_{k_0+1}\cos\omega + 2a_2 y_{k_0}\cos\omega - 2b_2 u_{k_0}\cos\omega \\ &\quad - a_1 y_{k_0} - a_2 y_{k_0-1} + b_1 u_{k_0} + b_2 u_{k_0-1}. \end{aligned} \tag{27}$$

Substituting for y_{k_0+1} and y_{k_0+2} in the 4th and 3rd terms in (27), using (15) and (16), respectively, and using (9) and (17) yields

$$\begin{aligned}\tilde{y}_{k_0+3} &= -a_1 y_{k_0+2} - a_2 y_{k_0+1} \\ &\quad + b_1 \sin\omega(k_0+2) + b_2 \sin\omega(k_0+1) \\ &= y_{k_0+3}. \end{aligned} \tag{28}$$

Using (12), (23), (26), (28), and setting $k = k_0 + 3$ in (19) yields

$$\begin{aligned}\tilde{y}_{k_0+4} &= -a_1 y_{k_0+3} - a_2 y_{k_0+2} + 2y_{k_0+3}\cos\omega - y_{k_0+2} \\ &\quad + 2a_1 y_{k_0+2}\cos\omega + 2a_2 y_{k_0+1}\cos\omega \\ &\quad - a_1 y_{k_0+1} - a_2 y_{k_0} + b_2 u_{k_0}. \end{aligned} \tag{29}$$

Substituting for y_{k_0+2} and y_{k_0+3} in the 4th and 3rd terms in (29), using (16) and (17), respectively, and using (9) and (17) yields

$$\begin{aligned}\tilde{y}_{k_0+4} &= -a_1 y_{k_0+3} - a_2 y_{k_0+2} \\ &\quad + 2b_1 \sin\omega(k_0+3) + b_2 \sin\omega(k_0+2) \\ &= y_{k_0+4}. \end{aligned} \tag{30}$$

Using (12), (23), (26), (28), (30), and setting $k = k_0 + 4 + p$, where $p \geq 0$ in (19), yields

$$\begin{aligned}\tilde{y}_{k_0+5+p} &= -a_1 y_{k_0+4+p} - a_2 y_{k_0+4+p} \\ &\quad + 2y_{k_0+4+p}\cos\omega - y_{k_0+3+p} \\ &\quad + 2a_1 y_{k_0+3+p}\cos\omega + 2a_2 y_{k_0+2+p}\cos\omega \\ &\quad - a_1 y_{k_0+2+p} - a_2 y_{k_0+1+p}. \end{aligned} \tag{31}$$

Substituting for y_{k_0+3+p} and y_{k_0+4+p} in the 4th and 3rd terms in (31), using (17), respectively, and using (9) and (17) yields

$$\begin{aligned}\tilde{y}_{k_0+5+p} &= -a_1 y_{k_0+4+p} - a_2 y_{k_0+3+p} \\ &\quad + b_1 \sin\omega(k_0+4+p) + b_2 \sin\omega(k_0+3+p) \\ &= y_{k_0+5+p}. \end{aligned} \tag{32}$$

Since $\tilde{y}_{k_0+5+p} = y_{k_0+5+p}$ for all $p \geq 0$, this completes the proof for $n = 2, n_\omega = 1$. □

V. A Numerical Example

Consider the SISO system (1) where G is given by

$$G(\mathbf{q}) = \frac{(\mathbf{q}^2 - 1.4\mathbf{q} + 0.58)(\mathbf{q}^2 - 0.4\mathbf{q} + 0.13)}{(\mathbf{q} - 0.7)(\mathbf{q}^2 - 0.8\mathbf{q} + 0.52)(\mathbf{q}^2 - 0.2\mathbf{q} + 0.5)}. \tag{33}$$

The true system (33) is driven by the sum of a Gaussian white-noise signal $u_k \sim \mathcal{N}(0, 10)$ and the unmodeled sum of sinusoids

$$w_k = \sin 0.5k + 0.8\sin 1.1k + 1.3\sin 1.5k. \tag{34}$$

The system (33) is simulated for $k \in [0, 1000]$, and samples of y_k and u_k are used to fit the coefficients of G. We use a recursive least squares technique (RLS) with variable rate forgetting (VRF) [10] to fit a model to the data. We choose an 11th-order model structure to account for the 5th-order system (33), and the disturbance (34), which is a sum of 3 sinusoids. The poles and zeros of the identified model are shown in Figure 3. As can be seen, the identified model correctly estimates the poles and zeros of the true system. Three pairs of complex conjugate poles on the unit circle with coincident zeros are also evident; these poles are at the frequencies of the unmodeled disturbance.

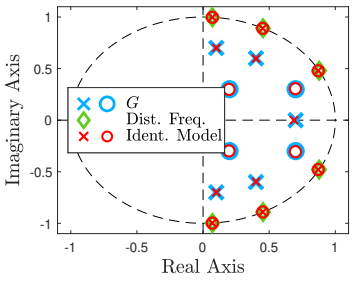

Fig. 3. Poles and zeros of the true system G, the disturbance frequencies, and poles and zeros of the identified model.

Next, we simulate the identified model and compare its response to the response of the true system. In particular, the identified model, without cancelling the spurious poles and zeros, is simulated with zero input. Therefore, the response $\tilde{y}_k$ of the identified model is given by its free response with initial y_k, u_k data obtained from a window of length 11 steps prior the end of the previous simulation. In addition, the true system is simulated with input consisting only of w_k; u_k is set to zero. Therefore, the response y_k of the true system is given by the sum of its free response and forced response

with initial $y_k, u_k + w_k$ data obtained from a window of length 5 steps prior the end of the previous simulation and with w_k applied at all subsequent steps. Figure 4 shows that the response of the identified model and true system are identical. This example numerically verifies Proposition 1 for $n = 5$ and $n_\omega = 3$. That is for the case where the system has order greater than 2, and the disturbance is a sum of multiple sinusoids of different amplitudes and frequencies.

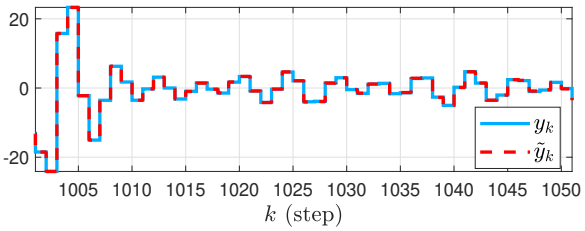

Fig. 4. This plot shows that the free response of identified model is identical to the free-plus-forced response of the true system. Note that, after the initial transients, which are identical, the steady-state harmonic responses are identical in frequency, amplitude, and phase.

VI. Application to Model Predictive Control

In this section we apply predictive cost adaptive control (PCAC) [6], which combines online identification using RLS and VRF with receding horizon optimization using quadratic programming (QP). The receding horizon optimization in PCAC utilizes the most recent model identified by RLS without removing coincident, spurious poles and zeros arising from the harmonic disturbance. The following example demonstrates the utility of these poles and zeros for harmonic disturbance rejection.

Consider the system

$$y_k = G_u(\mathbf{q})u_k + G_w(\mathbf{q})w_k, \tag{35}$$

where

$$G_u(\mathbf{q}) \triangleq \frac{\mathbf{q} - 0.4}{(\mathbf{q} - 0.6)(\mathbf{q} - 0.8)}, \tag{36}$$

$$G_w(\mathbf{q}) \triangleq -\frac{0.8(\mathbf{q} - 0.2)}{(\mathbf{q} - 0.6)(\mathbf{q} - 0.8)}. \tag{37}$$

State space realizations for these transfer function show that the disturbance w_k is unmatched to the control u_k. Let $w_k = \sin(0.35k) + 0.6\sin(0.8k + 0.1)$. The measurement y_k is corrupted by zero-mean, Gaussian white sensor noise with standard deviation 0.01 yielding a signal to noise ratio of approximately 44 dB. PCAC is applied with $u_{\min} = -5$, $u_{\max} = 5$, $\Delta u_{\min} = -10$, $\Delta u_{\max} = 10$, $\ell = 60$, $\bar{Q} = 10I_{\ell-1}$, $\bar{P} = 10$, $R = 0.01I_\ell$, $\eta = 0.05$, $\tau_{\mathrm{n}} = 60$, $\tau_{\mathrm{d}} = 200$, $\hat{n} = 10$, $\theta_0 = 10^{-2}1_{2\hat{n}\times 1}$, and $P_0 = 10^3 I_{2\hat{n}}$. Output constraints are not considered. Figure 5 shows that approximately coincident, spurious poles and zeros are identified on the unit circle, corresponding to the spectrum of w_k. Because of sensor noise, the closed-loop identification of G_u is poor [11]. However, the identified model correctly identifies coincident poles and zeros at the frequencies in the disturbance w_k. Figure 6 shows that, with this model, which is updated at each time step, the harmonic disturbance is asymptotically rejected. Consequently, the approximately coincident, spurious poles and zeros enable PCAC to reject the unmeasured, unknown, and unmatched two-tone harmonic disturbance.

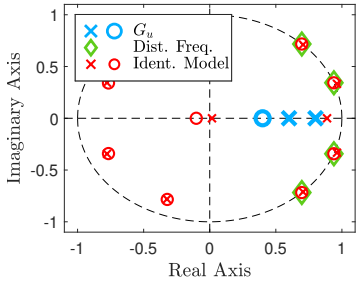

Fig. 5. Poles and zeros of G_u and the identified model at $k = 250$. Because of sensor noise, the closed-loop identification of G_u is poor. However, the identified model correctly identifies coincident poles and zeros at the frequencies in the disturbance w_k.

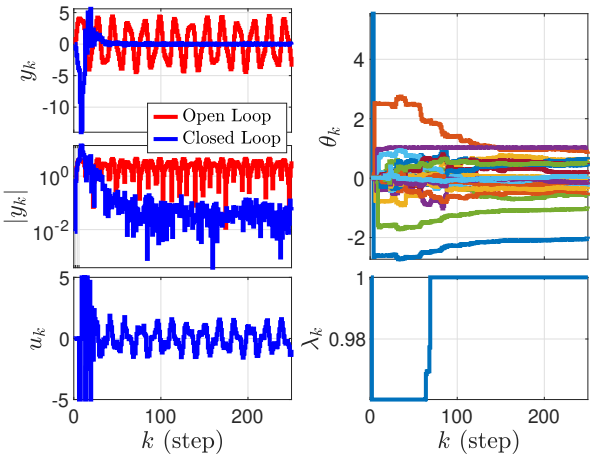

Fig. 6. Harmonic disturbance rejection using PCAC. The harmonic disturbance w_k is rejected asymptotically.

Next, in order to confirm that the approximately coincident, spurious poles and zeros on the unit circle are truly enabling disturbance rejection, we apply PCAC with fixed models that are identical to $G_u(\mathbf{q})$ and $G_w(\mathbf{q})$, which requires setting $\hat{n} = 2$.

Figures 7 and 8 shows that the use of the model without the approximately coincident, spurious poles and zeros on the unit circle within PCAC does not yield asymptotic harmonic disturbance rejection.

This numerical simulation shows that the presence of approximately coincident, spurious poles and zeros is beneficial even in the presence of an unmatched sinusoidal disturbance, in the presence of sensor noise, and with an overparametrizated model of the system. In particular, the identification of the spurious poles and zeros facilitates harmonic disturbance rejection within the framework of PCAC.

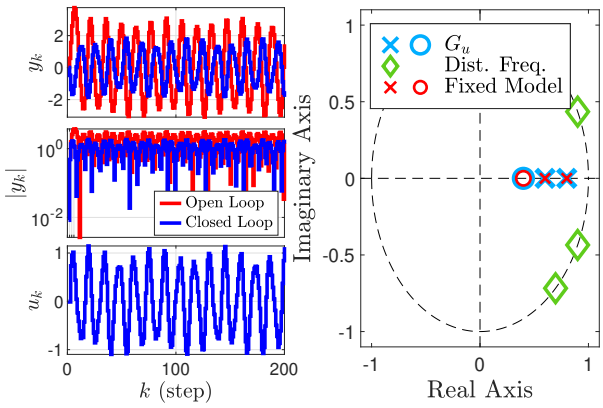

Fig. 7. Harmonic disturbance rejection using PCAC with a fixed model that is identical to $G_u(\mathbf{q})$. Asymptotic disturbance rejection is not achieved.

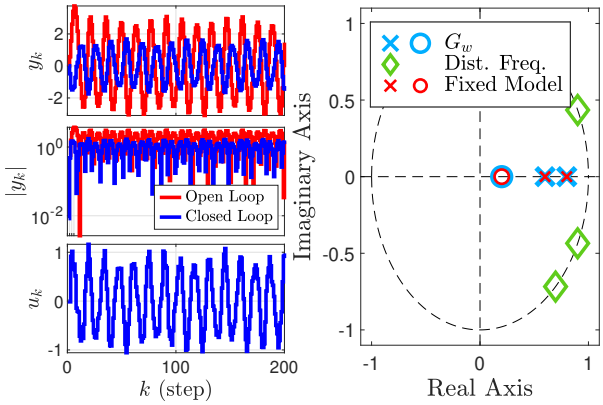

Fig. 8. Harmonic disturbance rejection using PCAC with a fixed model that is identical to $G_w(\mathbf{q})$. Asymptotic disturbance rejection is not achieved.

VII. Conclusions and Future Research

This paper described a surprising phenomenon arising from system identification in the presence of an unmodeled harmonic disturbance, namely, that the forced response of the true system is predicted by the free-plus-forced response of an identified model with the coincident, spurious poles and zeros at the disturbance frequency. This suggests that retaining the coincident, spurious poles and zeros has predictive value, thus contradicting the standard practice of cancelling coincident poles and zeros. This observation was encapsulated in Proposition 1, which was proved for first- and second-order systems with a single harmonic disturbance. This proof entailed the derivation of recursions for both systems. Future research will extend this proof through induction as well as extending this approach to MIMO systems.

References

[1] M. Kamaldar and J. B. Hoagg, "Adaptive Harmonic Control for Rejection of Sinusoidal Disturbances Acting on an Unknown System," *IEEE Trans. Contr. Sys. Tech.,*, vol. 28, no. 2, pp. 277–290, 2020.

[2] M. Bodson and S. C. Douglas, "Adaptive algorithms for the rejection of sinusoidal disturbances with unknown frequency," *Automatica*, vol. 33, no. 12, pp. 2213–2221, 1997.

[3] B. Francis and W. Wonham, "The internal model principle of control theory," *Automatica*, vol. 12, no. 5, pp. 457 – 465, 1976.

[4] T. W. Nguyen, S. A. U. Islam, A. L. Bruce, A. Goel, D. S. Bernstein, and I. V. Kolmanovsky, "Output-feedback rls-based model predictive control," in *Proc. Amer. Contr. Conf.*, 2020, pp. 2395–2400.

[5] N. Mohseni, T. W. Nguyen, S. A. U. Islam, I. V. Kolmanovsky, and D. S. Bernstein, "Active noise control for harmonic and broadband disturbances using rls-based model predictive control," in *Proc. Amer. Contr. Conf.*, 2020, pp. 1393–1398.

[6] T. W. Nguyen, S. A. U. Islam, D. S. Bernstein, and I. V. Kolmanovsky, "Predictive Cost Adaptive Control - A Numerical Investigation of Persistency, Consistency, and Exigency," *IEEE Contr. Sys. Mag.*, vol. 41, no. 6, 2021.

[7] K. F. Aljanaideh and D. S. Bernstein, "Initial Conditions in Time- and Frequency-Domain System Identification: Implications of the Shift Operator versus the Z Transform," *IEEE Contr. Sys. Mag.*, vol. 38, no. 2, pp. 80–93, 2018.

[8] S. A. U. Islam and D. S. Bernstein, "Recursive least squares for real-time implementation," *IEEE Contr. Sys. Mag.*, vol. 39, no. 3, pp. 82–85, 2019.

[9] D. S. Bernstein, *Scalar, Vector, and Matrix Mathematics: Theory, Facts, and Formulas—Revised and Expanded Edition*. Princeton University Press, 2018.

[10] A. L. Bruce, A. Goel, and D. S. Bernstein, "Recursive Least Squares with Matrix Forgetting," in *Proc. Amer. Contr. Conf.*, 2020, pp. 1406–1410.

[11] F. Sobolic, K. F. Aljanaideh, and D. S. Bernstein, "A numerical investigation of direct and indirect closed-loop architectures for estimating nonminimum-phase zeros," *Int. J. Contr.*, vol. 93, no. 6, pp. 1251–1265, 2020.